Journal of Hydrology 538 (2016) 374–386

Contents lists available at ScienceDirect

Journal of Hydrology

journal homepage: www.elsevier.com/locate/jhydrol

Evapotranspiration partitioning, stomatal conductance, and components of the water balance: A special case of a desert ecosystem in China

Wenzhi Zhao [a,*], Bing Liu [a,*], Xuexiang Chang [a], Qiyue Yang [a], Yuting Yang [b], Zhiling Liu [c], James Cleverly [d], Derek Eamus [d]

[a] Linze Inland River Basin Research Station, Laboratory of Heihe River Eco-Hydrology and Basin Science, Cold and Arid Regions Environmental and Engineering Research Institute, Chinese Academy of Sciences, Lanzhou 730000, China
[b] CSIRO Land and Water, Canberra, ACT, Australia
[c] School of Public Administration, China University of Geosciences, Wuhan 430074, China
[d] School of the Environment, University of Technology, Sydney, NSW, Australia

ARTICLE INFO

Article history:
Received 28 July 2015
Received in revised form 18 April 2016
Accepted 20 April 2016
Available online 27 April 2016
This manuscript was handled by Corrado Corradini, Editor-in-Chief, with the assistance of Magdeline Laba, Associate Editor

Keywords:
Evapotranspiration
Ecosystem water balance
Canopy transpiration
Soil evaporation
Stomatal conductance

SUMMARY

Partitioning evapotranspiration (*ET*) into its components reveals details of the processes that underlie ecosystem hydrologic budgets and their feedback to the water cycle. We measured rates of actual evapotranspiration (ET_a), canopy transpiration (T_c), soil evaporation (E_g), canopy-intercepted precipitation (E_l), and patterns of stomatal conductance of the desert shrub *Calligonum mongolicum* in northern China to determine the water balance of this ecosystem. The ET_a was 251 ± 8 mm during the growing period, while E_l, T_c, and E_g accounted for 3.2%, 63.9%, and 31.3%, respectively, of total water use (256 ± 4 mm) during the growing period. In this unique ecosystem, groundwater was the main water source for plant transpiration and soil evaporation, T_c and exceeded 60% of the total annual water used by desert plants. *ET* was not sensitive to air temperature in this unique desert ecosystem. Partitioning *ET* into its components improves our understanding of the mechanisms that underlie adaptation of desert shrubs, especially the role of stomatal regulation of T_c as a determinant of ecosystem water balance.

1. Introduction

Evapotranspiration (*ET*) is the largest process of ecosystem water loss and is a major determinant in the ecosystem water budget and energy balance (Law et al., 2002; Scott et al., 2006; Hu et al., 2009). In arid zones, *ET* can account for up to 95% of all water inputs (Wilcox and Thurow, 2006). Generally, *ET* is the aggregate of water loss measured using micrometeorological techniques and soil parameters and does not distinguish the pathway and components of water loss. In contrast, actual evapotranspiration (ET_a) is composed of and estimated by several of the *ET* components, including the linked vapor fluxes of canopy transpiration (T_c), soil evaporation (E_g), and canopy-intercepted precipitation (E_l) (Mitchell et al., 2009; Raz-Yaseef et al., 2012). As a consequence, ET_a can partition *ET* into its component fluxes, thereby contributing to our understanding of the relative controls of T_c *versus* E_g (Lawrence et al., 2007; Wang et al., 2010) and helping to resolve the critical uncertainties regarding the coupling of water and energy cycles in arid regions (Austin et al., 2004; Breshears, 2006; Wang et al., 2010). While partitioning *ET* involves the use of multiple technologies, including lysimeters, sap flow sensors, infrared thermometers, stable isotopes (Scott et al., 2006; Morana et al., 2009), and modeling (Reynolds et al., 2000; Hu et al., 2009), such studies remain both an observational and theoretical challenge (Huxman et al., 2005; Caylor et al., 2006; Morana et al., 2009; Wang et al., 2010), particularly in terms of scaling from whole-plant to ecosystem levels in arid regions. Therefore, the aim of this work was to provide independent measurements of *ET* and its components at different scales in order to unravel details of the processes that underlie ecosystem hydrologic budgets and feedback in a unique desert ecosystem in arid regions.

Global warming may increase the variability in precipitation and the likelihood of drought conditions, including within arid regions (Dai, 2011). Consequently understanding the partitioning of *ET* will become increasingly important for sustainable management of water resources at regional scales. Partitioning of *ET* has been intensively studied globally (e.g., Lei and Yang, 2010; McCulloh and Woodruff, 2012; Kool et al., 2014; Mendez-Barroso

* Corresponding authors. Tel.: +86 931 4967137.
E-mail addresses: zhaowzh@lzb.ac.cn (W. Zhao), liubing@lzb.ac.cn (B. Liu).

http://dx.doi.org/10.1016/j.jhydrol.2016.04.042
0022-1694/

et al., 2014). The ratio T_c/ET varies greatly among ecosystems and timescales (Mitchell et al., 2009; Morana et al., 2009; Cavanaugh et al., 2010; Staudt et al., 2011) so that *ET per se* is often not a good indicator of productivity (i.e., contributing to vegetation carbon gain). These studies indicate that the ratio T_c/ET reflects forest productivity and survival in semi-arid ecosystems and is controlled by canopy conductance and leaf area index (LAI) (Hu et al., 2009; Mendez-Barroso et al., 2014). T_c is the dominant component of *ET* across a variety of ecohydrological ecosystems (Williams et al., 2004; Eamus et al., 2006) and is determined by interactions among plant physiology, environmental conditions, and stomatal regulation (Peters et al., 2010; Raz-Yaseef et al., 2012; Litvak et al., 2012). However, many such studies have failed to accurately measure E_l because scaling from individual measures of transpiration to an ecosystem scale remains problematic.

The sensitivity of stomata to atmospheric water deficits varies significantly among species (Oren et al., 1999a,b; McCulloh and Woodruff, 2012). The sensitivity of stomata to vapor pressure deficit (*VPD*) can be quantified as the magnitude of the response of stomatal conductance to increasing *VPD* relative to two reference conductances, one at *VPD* = 1 kPa and the second at the *VPD* that induces stomatal closure (Meinzer et al., 1997; Oren et al., 1999a, b). While stomatal closure prevents the failure of the water-conducting pathway in xylem arising from the formation of emboli, it also reduces photosynthetic rates—a trade-off that has important implications for plant function and growth, particularly under drought stress (Wullschleger et al., 2002; Addington et al., 2004). Thus, stomatal regulation of transpiration can improve water-use efficiency of vegetation and influences the productivity of terrestrial ecosystems (Maherali et al., 2003; McDowell et al., 2008). However, stomatal sensitivity to changes in T_c at canopy scales also varies greatly with a wide range of stomatal behaviors within and between species (Oren et al., 1999a,b). Currently, quantifying stomatal sensitivity can be performed using long-term field campaigns at the leaf and canopy levels (Bush et al., 2008; Peters et al., 2010), but predicting stomatal sensitivity based on hydraulic properties of plants remains a major challenge (Maherali et al., 2003; Litvak et al., 2012). Clearly there is a need for further quantification of stomatal sensitivities at canopy and community scales to improve our understanding and predictive ability of the patterns of T_c and *ET* at an ecosystem scale.

The desert–oasis ecotone is unique in arid regions of China where it plays an important role in preventing the movement of sand dunes and maintaining the ecosystem structure and function and hydrological balance (Liu and Zhao, 2009; Zhao and Liu, 2010; Liu et al., 2011). It is therefore also an important component of the desert–oasis ecosystem. Because rainfall is rare in this region, the uniqueness of the desert–oasis ecotone lies in the water resource derived from shallow groundwater and the seepage of river and farmland irrigation, and water is consumed through vegetation transpiration and soil evaporation. Consequently, the ecohydrologic processes result in discontinuous patterns of plaque distribution of vegetation, so this ecosystem is sensitive to changes in hydrologic processes (Zhao and Chang, 2014). However, few studies in China have partitioned *ET* or determined the components of ecosystem water balance, particularly in a desert ecosystem where the vegetation can utilize the shallow groundwater table. We therefore measured the T_c, E_g, E_l, and ET_a of a unique desert–oasis ecosystem of China. Our specific objectives were (1) to scale from whole-plant transpiration to the community level; (2) to partition *ET* into components of ecosystem water balance; (3) to examine the influence of stomatal regulation of T_c, and *ET* at canopy and community scales; and (4) to determine the effects of plant physiology and environmental conditions on the components of *ET* and on stomatal conductance. Such information will contribute to our understanding of the effects of climate change on the water resources of a unique desert ecosystem.

2. Materials and methods

2.1. Study area

Our study site is located in a desert–oasis ecotone in the middle of China's Heihe River Basin (between 39°21′N and 39°24′N, and between 100°06′E and 100°09′E; Fig. 1). The region has a continental and arid temperate climate. Annual rainfall averages 116.8 mm, of which about 65% falls between July and September. Annual temperature averages 7.6 °C and ranges from a minimum of −27.3 °C in January to a maximum of 39.1 °C in July. The growing season lasts from May to October, and the frost-free period is about 165 days. The zonal desert soil is characterized as unconsolidated sand with a high variability in soil thicknesses and grain sizes (grains between 0.05 and 0.25 mm in diameter account for 80–90% of the total) and low vegetation cover, which ranges from 15% to 20% and is highly susceptible to wind erosion (Zhao and Liu, 2010). The landscape is dominated by fixed and semi-fixed dunes that are separated by inter-dune lowlands. Vegetation comprises desert shrubs that are found on the fixed dunes and in the inter-dune lowlands, including *Calligonum mongolicum* and *Nitraria sphaerocarpa*. Annual herbs include *Bassia dasyphylla*, *Halogeton arachnoideus*, *Suaeda glauca*, and *Agriophyllum squarrosum*, which

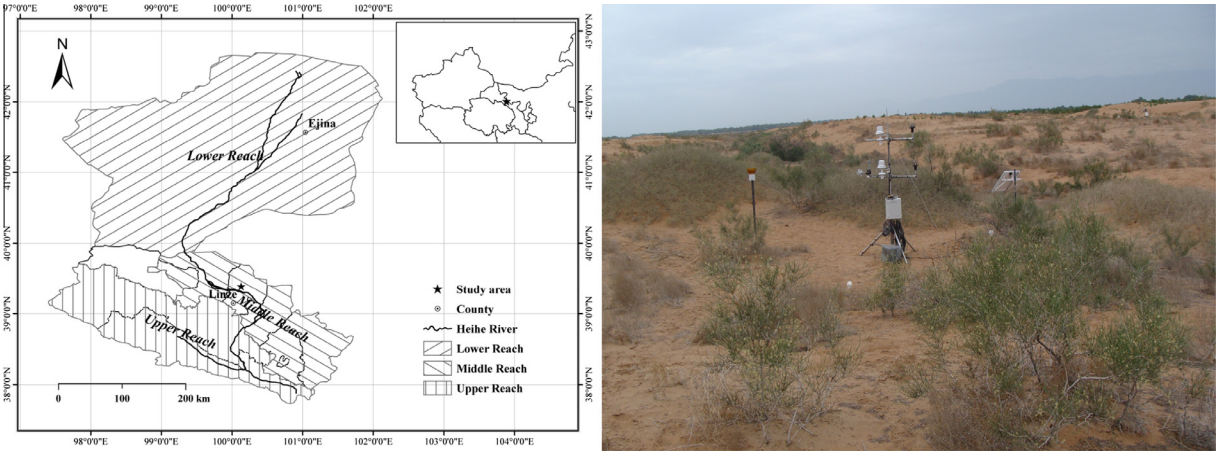

Fig. 1. Map of the study area and location in China.

are common components of desert vegetation ecosystems in arid regions of China.

2.2. Measurements

2.2.1. Vegetation measurements

The experiments were conducted in the inter-dune area between fixed dunes during the growing seasons from 2008 to 2010. A sample area of *C. mongolicum* community (100 m × 100 m) was selected within which all vegetation and sap flow measurements were conducted. Following a vegetation survey to determine species composition, basal diameter, canopy area, plant height, and stem density during the growing season across the entire plot, we selected *C. mongolicum* as the dominant species based on the abundance of shrubs. Every 10 days during each growing season for a total of 100 days, the leaf area index (LAI) that represented the area vegetation cover was measured across the 1-ha plot, using a plant canopy analyzer (LAI-2000, Li-Cor Inc., Lincoln, NE, USA). Table 1 summarizes the results of these measurements.

2.2.2. Canopy interception measurements

Rainfall was partitioned into throughfall, stemflow, and canopy interception by *C. mongolicum* under the natural precipitation regime in the study area. Precipitation was measured with a tipping-bucket rain gauge (model TE525, metric; Texas Electronics, Dallas, TX, USA) located in a large clearing, and the data were stored as 10-min means. Stemflow and throughfall were measured for 80 individual plants following the method described by Liu and Zhao (2009) and summarized below.

We chose 12 individual shrubs for measurements of stemflow. Data were collected using plastic funnels fitted around the main stems and sealed with silicone sealant. Each funnel was connected via plastic tubes to a collecting bottle where the stemflow was stored. Stemflow volumes for each plant were divided by its projected canopy area occupied by these shrubs and then totaled for the whole study site to calculate stemflow, expressed as water depth. Throughfall was collected using 36 plastic containers, with each container established under the canopy of the sample shrubs around separate stems. The containers were established in three concentric rings of four containers at 33%, 67%, and 100% of the crown width to permit the sampling of how different crown densities affected the results. Throughfall and stemflow depth within each container were measured within 3 h after precipitation or after sunrise if the event occurred or extended into nighttime hours, thereby minimizing evaporative losses from the containers. Throughfall depth was measured with the same type of measuring cup used to measure stemflow depth (Liu and Zhao, 2009). Canopy interception (E_I, mm) was estimated by the following relationship (Liu and Zhao, 2009):

$$E_I = P - TF - SF, \tag{1}$$

where P is precipitation (mm), TF is throughfall (mm), and SF is stemflow (mm).

2.2.3. Soil evaporation, soil moisture, and groundwater measurements

Soil evaporation was measured using micro-lysimeters with a diameter of 30 cm and a height of 30 cm. We installed a micro-lysimeter at distances of 50, 100, and 150 cm east, north, west, and south of each of five individuals of *C. mongolicum* (for a total of 12 per plant). The micro-lysimeters were weighed at 19:00 every day using a two-figure electronic balance (PL 6001-L; Mettler Toledo Inc., Greifensee, Switzerland). Soil in the micro-lysimeters was replaced every 5–7 days or replaced after heavy rains. We calculated E_g (mm d^{-1}) using the following formula:

$$E_g = 10 \times \left(\frac{\Delta W / \rho_w}{\pi (D/2)^2} \right) \tag{2}$$

where ΔW is the difference in weight (g), ρ_w is the density of water (g cm^{-3}), and D is the diameter of the micro-lysimeter.

Volumetric soil water content was measured using 40 ECH_2O-10 dielectric probes (Decagon Devices, Pullman, WA, USA) buried at eight depths below the soil surface (10, 20, 30, 40, 50, 60, 80, and 100 cm) across five replicate profiles within the 1-ha plot. Soil water content was measured every 10 days by means of oven drying to validate the soil moisture data provided by the dielectric probes during the study period; the accuracy was over 90.5%. Simultaneously, depth to the water table was measured automatically within five observation wells (5 cm diameter PVC pipe) using a water-level sensor (HOBO; Onset Computer Corporation, USA). Soil moisture and depth to the water table data were stored every hour.

2.2.4. Measurements of sap flow and estimations of stand transpiration

To estimate canopy transpiration, we continuously measured sap flow of *C. mongolicum* with stem flow gauges (Flow32; Dynamax Inc., TX, USA) from May to October (2008 to 2010). The gauges, which had diameters of 3 (SGB3), 5 (SGB5), 9 (SGB9), 13 (SGB13), and 19 (SGB19) mm, were located just above the soil surface on each stem and had three replicates in each size class. The data were recorded at 10-s intervals and stored as 30-min averages using a CR1000 data logger (Campbell Scientific, Logan, UT, USA).

At the study site, canopy transpiration (T_c, mm day^{-1}) was estimated from sap flow measurements using the following equation (Yue et al., 2008):

$$T_c = \sum_{i=1}^{n} \frac{1000 F_i}{A_i \rho_w} \times A \tag{3}$$

where n is the number of gauged stems, A_i is the basal area through which water transfer occurs in the plant, A is the basal cross-sectional area per ground area (cm^2 m^{-2}) or LAI (m^2 m^{-2}), F_i is the sap flow measured in stem i (kg day^{-1}), and ρ_w is the density of water (g cm^{-3}).

Canopy conductance (or stomatal conductance at the canopy scale; g_c, mm s^{-1}) was estimated from canopy transpiration as (Chang et al., 2006; Granier et al., 1996; Monteith and Unsworth, 1990)

$$g_c = \frac{\lambda T_c \gamma}{p c_p VPD} \tag{4}$$

where λ is the latent heat of vaporization of water (2465 kJ kg^{-1}), γ is the psychrometric coefficient (65.5 Pa K^{-1}), p is the air density (1.225 kg m^{-3}), c_p is the specific heat of dry air (1.01 kJ kg^{-1} K^{-1}), and VPD is vapor pressure deficit (kPa) measured between 1 and 2 m above the canopy.

Table 1
The morphological characteristics of *C. mongolicum* at the study site during the growing seasons. Values are mean ± SD (n = 300).

Species	Height (m)	Canopy height (cm)	Basal diameter (mm)	Crown length (m)	Canopy area (cm^2)	LAI (m^2 m^{-2})
C. mongolicum	1.2 ± 0.4	18.8 ± 4.2	12.4 ± 6.6	0.6 ± 0.2	6.2 ± 0.2	1.0 ± 0.5

2.2.5. Meteorological measurements and evapotranspiration calculations

Meteorological data were measured using an BREB (Bowen ratio energy-balance) systems (Onset Computer Corporation) at *C. mongolicum* community in the study site, over a large area of desert shrubs and approximately 15 km from the oasis. The sensors for wind speed, air temperature and humidity, atmospheric pressure, and water vapor were installed at two levels above the canopy (1 and 2 m). The sensors for net radiation and photosynthetically active radiation were installed at 1 m above the canopy. Net radiation was measured with a closed-cell thermocouple sensor (NR-lite, Kipp and Zonen, Delft, the Netherlands). Air temperature and relative humidity were measured with an HMP45D probe (Vaisala, Vantaa, Finland). Atmospheric pressure and water vapor were measured using a barometric pressure sensor (CS100; Campbell Scientific). We buried three soil heat-flux plates (model HFP01; Campbell Scientific) at a depth of 1.5 cm in 1×1 m plots near the base of the meteorological tower but with a 10-m separation between plots. Data were measured at a frequency of 10 Hz and recorded every 5 min using a CR1000 data logger, then stored as the 30-min mean.

The accuracy of the calculated values of latent and sensible heat fluxes depends on the accuracy of the Bowen ratio, which in turn depends on the accuracy of the measurements. The BREB systems are susceptible to systematic errors if proper mutual sensor calibration is not carried out. In order to improve the sensors' accuracy when the gradient measurements, the capacitive non-alternating hygrometers have been successfully analyzed and validated by the professional engineers who come from the instrument manufacturers. Most systematic errors were eliminated through the sensor calibration in our laboratory by the engineers. As a result, the sensors' accuracy is guaranteed through the mutual sensor calibration to less than 0.2 °C for temperature measurements, 0.5% for relative humidity, and 18 Pa for vapor pressure, respectively. The accuracy of the measurement were checked annually to rule out any drift effect of the sensors by the professional engineers. Simultaneously, the same BREB system was installed at another plots where had the distance of about 350 m with the first system, to simultaneously measure the water and energy exchange of *N. sphaerocarpa* community from 2008 to 2010. And two BREB systems both were installed by the professional engineers with the same installation method and technical requirements. In fact, there are no significant differences in net radiation, air temperature and soil heat flux between two BREB systems with the pairs of similar covers under the same environment, so we mutually calibrated all data of net radiation, air temperature and soil heat flux to judge the reliability between two BREB systems throughout the study period.

The quality control of all measured data used the method of comparison on the premise of independent measurement (Allen et al., 2011a,b), by comparison with two BREB systems to evaluate consistency in measurements. The quality control were followed by several post-processing steps based on Fisher et al. Generally, the data were replaced in the corresponding period from another BREB system if the data did not meet the quality control (less than 3%), or were rejected when the data from another BREB system nor obey the quality requirements (The removed data was less than 5%): when (i) the energy fluxes with the wrong signs (i.e., those that did not obey the flux–gradient relationship), (ii) $\lambda ET > 100$ W m^{-2} or $\lambda ET < -100$ W m^{-2}, (iii) the Bowen ratio fell between -1.3 and -0.7 (Unland et al., 1996; Kurc and Small, 2004; Ma et al., 2015), and (iv) values exceeded the Perez et al. (1999) criteria for determining the suitable sign of λET (latent heat flux). Secondly, the data were excluded when the data obtained during rain events (less than 7%). Theoretically, the period of the missing data were less than a month because we collected the data once a month, so the missing data were timely discovered and all problems were solved. The gaps in data resulted only in 2009 (10 August to 28 August) because the wire was broken after precipitation. The half-hourly data was gap-filled by replacement in the corresponding period from another BREB system (less than 3%) or were rejected (less than 1%). Finally, the *ET* were plotted between two BREB systems during the growing period, and they were also plotted against the actual evapotranspiration ($ET_a = T_c$ (transpiration) + E_l (canopy interception) + E_g (soil evaporation)) from the field measurements and linear interpolation was parameterized between the values adjacent to the inconsistent value based on ET_a when data were nor obey the quality requirements for the two both BREB systems (The data was less than 2.4%). All the processes of quality control, the exclusion eventually comprised 15.4% of the total number of all BREB data, and all replacement by another BREB system accounted for 6% of all data. The accuracy of all data by the estimation of relative error was over 78.6%.

The BREB method was estimated evapotranspiration based on water energy exchange and the theory of turbulent diffusion (K-theory). The energy balance equation is as follows (Fischer et al., 2013):

$$Rn = \lambda ET + H + G + S + P \tag{5}$$

where R_n is the net radiation (W m^{-2}), λET is the latent heat flux (W m^{-2}), H is the sensible heat flux (W m^{-2}), G is the soil heat flux density (W m^{-2}), S is the rate of heat storage in the soil (W m^{-2}), and P is the rate at which energy is being trapped in chemical bonds by photosynthesis (W m^{-2}). P can be neglected since the since it is generally considered negligible compared to Rn (Lindroth and Iritz, 1993; Fischer et al., 2013).

The Bowen ratio (β) is calculated from gradients of temperature and vapor pressure measured at two heights above the canopy. Using the flux-gradient approach, assuming that K_h is equal to K_w, and $(\partial T/\partial z)/(\partial e_a/\partial z) \approx \Delta T/\Delta e_a$, The Bowen ratio is defined as follows:

$$\beta = \gamma \frac{\Delta T}{\Delta e_a} \tag{6}$$

where ΔT and Δe_a are the differences in temperature (°C^{-1}) and vapor pressure (kPa), respectively, between 1 and 2 m above the canopy.

We used the Bowen ratio energy-balance method to measure ecosystem evapotranspiration (*ET*), using the following equation (Fischer et al., 2013):

$$ET = \frac{1}{\lambda}\left(\frac{R_n - G - S - P}{(1+\beta)}\right) \tag{7}$$

To account for the rate of heat storage in the soil (S) between the soil heat flux plates and the surface, S was calculated as (Blanken, 2014):

$$S = C_s \frac{dT_s}{dt} dz \tag{8}$$

where C_s is the soil's volumetric heat capacity (J m^{-3} °C^{-1}), dT_s/dt is the change in soil temperature (T_s) over the 1800s time interval (t), and dz is the depth of the soil heat flux plates. The C_s was calculated as:

$$C_s = p_s C_d + p_w C_w \theta \tag{9}$$

where ρ_s is the measured dry soil bulk density (1590 kg m^{-3}), C_d is the estimated dry soil specific heat (840 J kg^{-1} °C^{-1}), ρ_w is the density of liquid water (997 kg m^{-3}), and C_w is the water specific heat (4190 J kg^{-1} °C^{-1}). θ is volumetric liquid soil moisture.

Community conductance, considered as stomatal conductance at the community scale (g_s, mm s^{-1}), was estimated by inverting the Penman–Monteith equation at the community scale:

$$g_s = \frac{\gamma L e g_a}{\Delta(Rn - G) + \rho C_p \Delta e_a - Le(\Delta + \gamma)} \quad (10)$$

where Le is the latent heat flux (W m^{-2}), g_a is the aerodynamic conductance (m s^{-1}), and Δ is the slope of the curve for saturation water vapor pressure as a function of air temperature (kPa °C^{-1}).

The decoupling coefficient (Ω) was obtained by the equation (Jarvis and McNaughton, 1986; Zhu et al., 2014).

$$\Omega = \frac{\Delta + \gamma}{\Delta + \gamma(1 + g_a/g_s)} \quad (11)$$

Bulk surface conductance for water vapor (G_s, m s^{-1}) was estimated by re-arranging the Penman–Monteith combination model as (Takagi et al., 1998)

$$G_s = \frac{1}{\frac{S(R_n - G)/g_a + pc_p VPD}{\gamma Le} - \frac{(S + \gamma)}{\gamma g_a}} \quad (12)$$

where S is the slope of the saturation vapor pressure–temperature curve at the mean wet-bulb temperature (kPa °C^{-1}).

2.2.6. Soil water balance

Surface runoff and deep percolation were negligible at our study site because annual precipitation is low and the infiltration rate into the sandy soil is high. Therefore, the soil water balance for the plot was estimated by the incoming and outgoing flux of water into the root zone during the study period as (Allen et al., 1998)

$$P - ET_a - GW_r = \Delta SWC \quad (13)$$

where P is precipitation (mm), ET_a is actual evapotranspiration (mm), ΔSWC is soil water storage (mm), and GW_r is groundwater use by vegetation (mm).

Actual evapotranspiration (ET_a, mm) was partitioned into three components: transpiration from the canopy (T_c, mm), canopy interception of precipitation (E_l, mm), and soil evaporation (E_g, mm):

$$ET_a = T_c + E_l + E_g. \quad (14)$$

2.3. Statistical analysis

We used SPSS software version 13.0 (SPSS Inc., Chicago, IL, USA) to analyze the significance in effects of environmental variables on T_c, g_c, ET, g_s, and E_g, using repeated-measures analysis of variance (ANOVA) to compare the main effects and the interaction effects of T, VPD, SWC, and R_n. We also performed one-way ANOVA and Tukey's HSD test (after testing for homogeneity of variance and confirming a normal distribution) to test for seasonal differences in the components of the water balance during the growing period. Values were considered to be significantly different at $P < 0.05$. We determined the regression equation by means of linear or nonlinear regression using version 8.6 of OriginPro software (www.OriginLab.com).

Nonlinear regression was used to estimate the coefficients of the equations for g_s and g_c as a function of VPD, T_c, and ER, which have the following form: $-m\ \ln(VPD)$ or $-m\ \ln(T_c/ET) + b$ (Oren et al., 1999a), where m describes the stomatal sensitivity to VPD or T_c/ET, b is the reference conductance at $VPD = 1$ kPa or $T_c/ET = 1$ mm d^{-1}, and $e^{b/m}$ is the extrapolated VPD or T_c/ET at which the stomata are completely closed.

3. Results and analyses

3.1. Meteorological and hydrological variables

The seasonal pattern of air temperature (T) was similar to vapor pressure deficit (VPD), R_n and G during the growing period from May to October (Fig. 2A–D). T increased from May to reach its maximum value in July and then decreased to its minimum value in October; its monthly average for the three growing seasons was 20.1 °C (Fig. 2A). VPD averaged 0.9 kPa, with maximum and minimum values of 1.2 and 0.6 kPa, respectively (Fig. 2B). G increased with increasing R_n, with maximum values of R_n and G in June and minimum values in October; average values were 76.9 (R_n) and 6.8 W m^{-2} (G), respectively (Fig. 2C and D).

Groundwater depth increased significantly from May, reaching a maximum of 5.7 m in August; its average depth over the three growing seasons was 5.2 m (Fig. 2E). SWC ranged from 1.3% to 2.7% and displayed the opposite trend to that of groundwater depth. Soil water content increased rapidly following each precipitation event (Fig. 2F). Precipitation mainly concentrated in July, August, and September and averaged 16.8 mm per month, with maximum and minimum values of about 50.6 mm and 5.5 mm (Fig. 2G). The annual rainfall averaged 113.3 mm, with the following distribution of rainfall: ⩽5 mm, 46.7% of annual rainfall and 56.1% of the events; 5.1–10 mm, 27.7% and 18.0%, respectively;

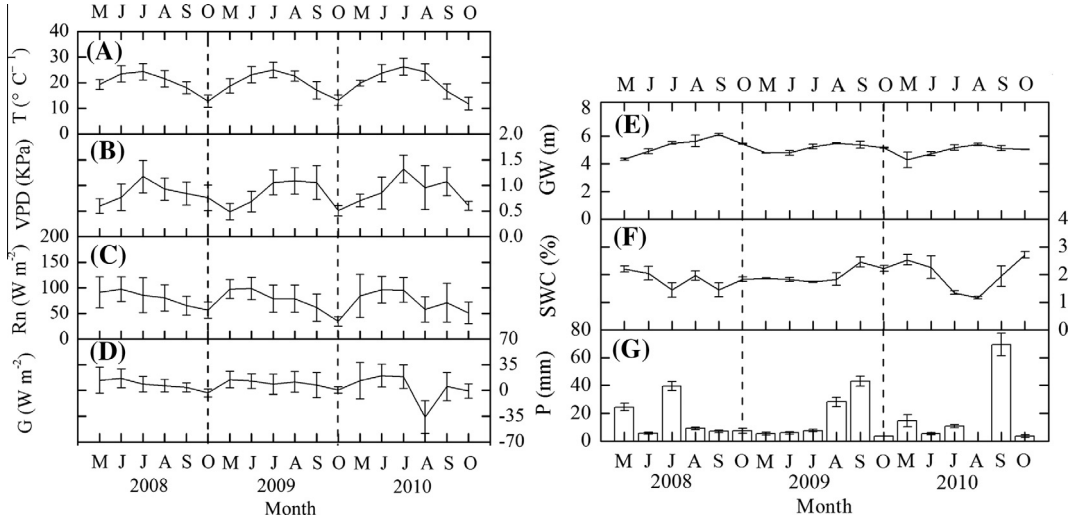

Fig. 2. Seasonal patterns of meteorological and hydrological variables during the growing period: (A) air temperature, T; (B) vapor pressure deficit, VPD; (C) net radiation, R_n; (D) soil heat flux density, G; (E) groundwater depth, GW; (F) soil water content, SWC; and (G) precipitation, P.

10.1–15 mm, 13.0% and 3.6%; 15.1–20 mm, 4.8% and 2.7%; 20.1–25 mm, 2.8% and 0.9%; and >25 mm, 5.0% and 18.7% (Zhao and Liu, 2010).

3.2. Seasonal and inter-annual variations in evapotranspiration partitioning and stomatal conductance

Canopy transpiration (T_c) displayed a distinct seasonal pattern that was in good agreement with that of *ET* and E_g (Fig. 3). T_c increased from May to reach its maximum in July, then gradually decreased during the remainder of the growing season. T_c ranged from 7.5 to 38.7 mm month^{-1} with an average of 27.2 mm month^{-1} (Fig. 3A). Rates of *ET* averaged 34.2 mm month^{-1} and ranged from 12.4 to 48.4 mm month^{-1} (Fig. 3C). However, E_g was relatively low with an average value of 13.0 mm month^{-1}, reaching a maximum of 1.8 mm d^{-1} after a large rainfall (Fig. 3D). The annual mean T_c was significantly lower in 2010 compared to 2008 and 2009, while E_g was significantly higher in 2010 compared to the other years. On the other hand, *ET* was significantly higher in 2008 compared to 2009 and 2010 ($P < 0.05$; Fig. 4A). E_I ranged from 0.3 to 5.6 month^{-1}, with an average of 1.3 month^{-1} (Fig. 3B), and differences among the three years were not significant (Fig. 4A).

T_c increased significantly as *ET* increased ($R^2 = 0.94$, $P < 0.001$; Fig. 5A), and there was a significant quadratic relationship between T_c and E_g ($R^2 = 0.81$, $P < 0.001$; Fig. 5B). In addition, E_g increased exponentially with increasing *ET* ($R^2 = 0.97$, $P < 0.001$; Fig. 5A).

Although g_c and g_s represent stomatal conductance at different scales (canopy and community, respectively), the seasonal pattern of g_c was in agreement with that of g_s, and both reached their maximum value in September or October, with average values of 211.6 and 278.0 mm s^{-1}, respectively (Fig. 3E and F). g_c in 2009 was significantly lower than in 2008 and 2010 ($P < 0.05$), whereas g_s did not differ significantly among the three years (Fig. 4B). As expected, g_s was significantly linearly correlated with g_c ($R^2 = 0.78$, $P < 0.001$; Fig. 5C). Similarly, bulk surface conductance (G_s) was significantly linearly correlated with g_s ($R^2 = 0.69$, $P < 0.001$), with a slope of 10.28 (Fig. 5D).

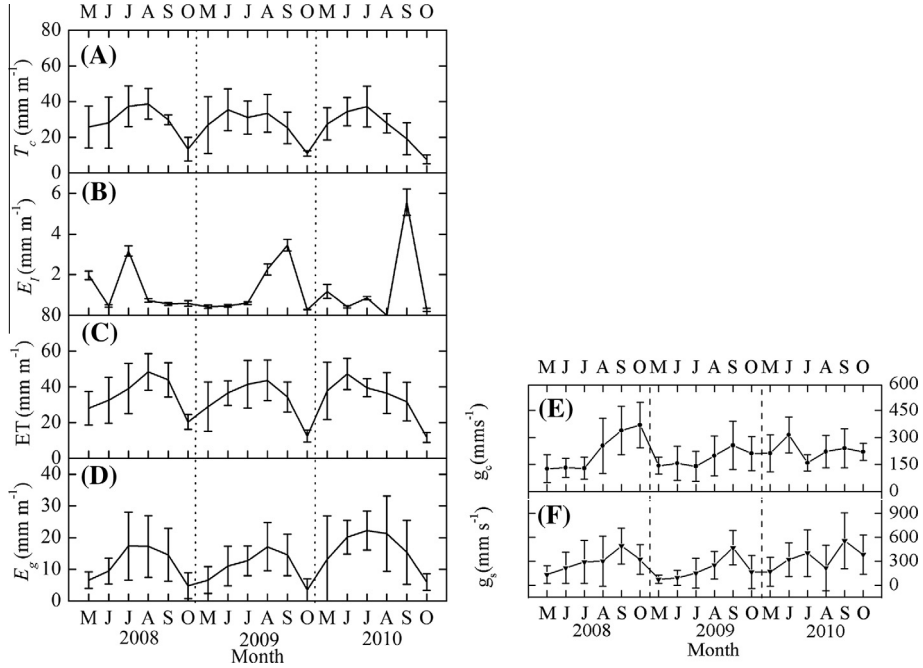

Fig. 3. Seasonal and inter-annual variation in mean monthly course of (A) canopy transpiration, T_c; (B) canopy interception, E_I; (C) evapotranspiration, *ET*; (D) soil evaporation, E_g; (E) canopy conductance, g_c; (F) community conductance, g_s.

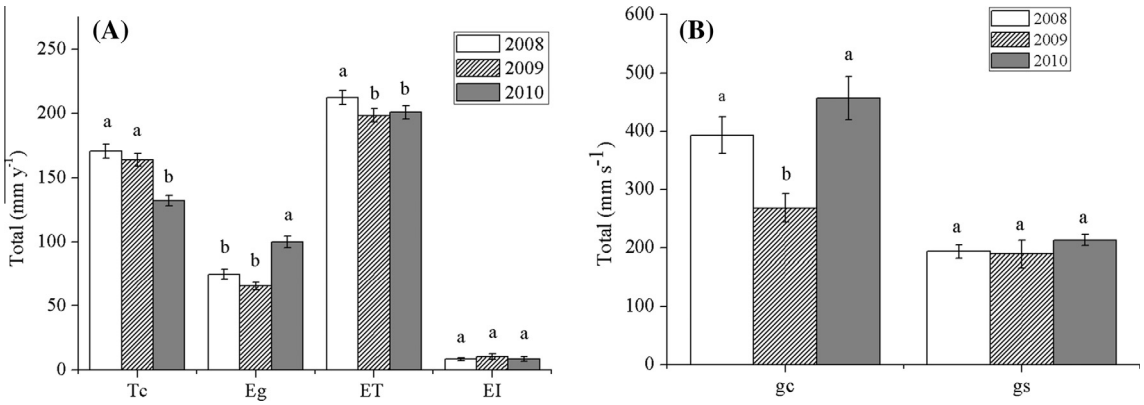

Fig. 4. Inter-annual rates of (A) canopy transpiration (T_c), soil evaporation (E_g), evapotranspiration (*ET*), and canopy interception (E_I) and (B) canopy conductance (g_c) and community conductance (g_s). Values of a parameter (±SEM) labeled with different letters differ significantly between years (Tukey's HSD, $P < 0.05$).

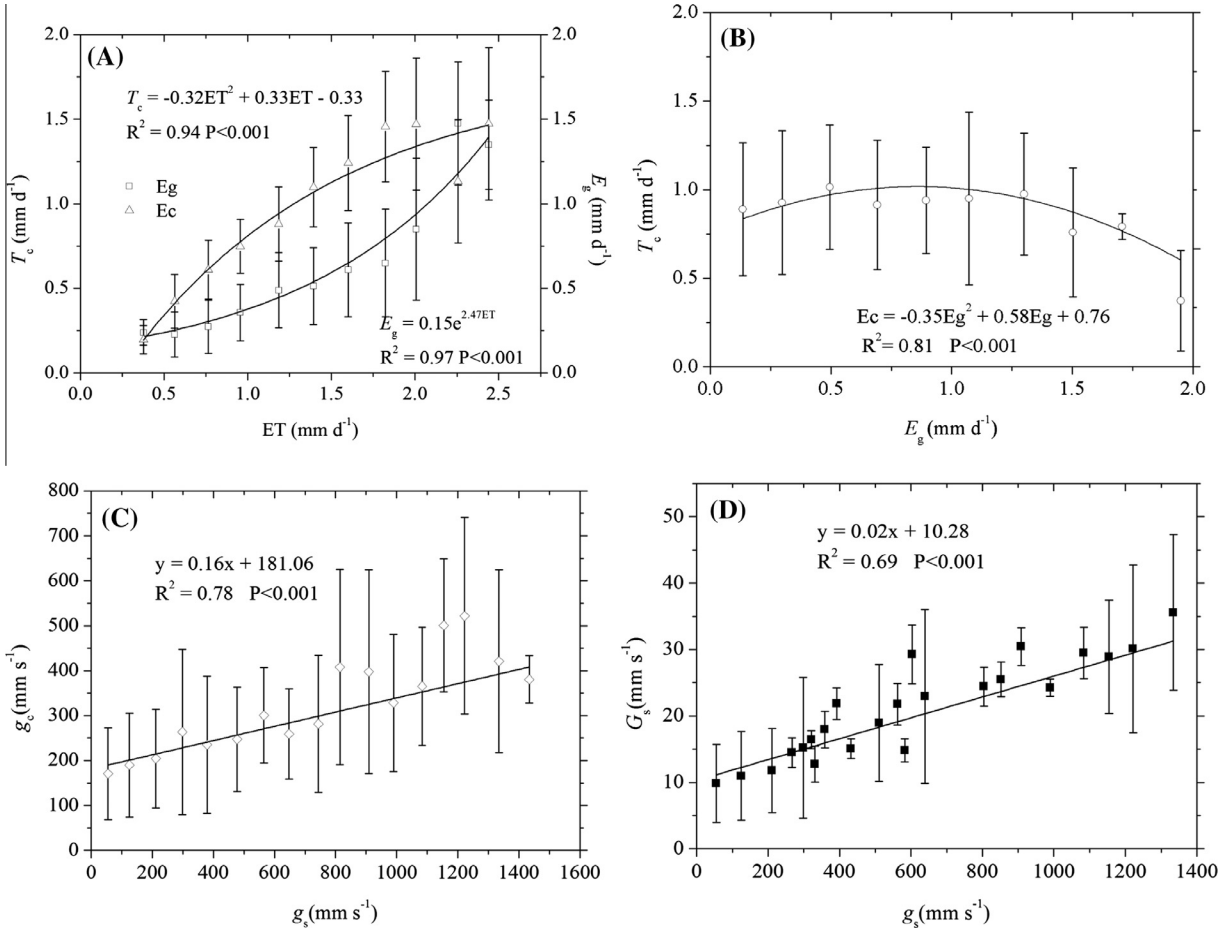

Fig. 5. The relationships between (A) evapotranspiration (*ET*), canopy transpiration (T_c) and soil evaporation (E_g); (B) canopy transpiration (T_c) and soil evaporation (E_g); (C) canopy conductance (g_c) and community conductance (g_s); and (D) bulk surface conductance (G_s) and community conductance (g_s).

Partitioning of rainfall showed that *TF*, *SF*, and E_l by *C. mongolicum* accounted for 83.5%, 8.5%, and 8.0% of the total rainfall, respectively. The relationships between *P* and *SF* were highly significant and parabolic (R^2 = 0.87, P < 0.01), whereas there was a significant linear relationship between *P* and *TF* (R^2 = 0.88, P < 0.01) and between *P* and E_l (R^2 = 0.90, P < 0.01) (Fig. 6).

3.3. Components of the water balance

The average annual *P* was 111 ± 9 mm for the three years, which accounted for 39.4% of the water consumed by the ecosystem (because of the utilization of groundwater; see below) during the growing period from May to October. There was a clear seasonal distribution in precipitation, with a significantly larger amount in September compared to other months.

Annual ET_a averaged 251 ± 8 mm and accounted for 98.3% of total water consumption (W_c) during the growing period; this was slightly greater than *ET* based on the Bowen ratio energy-balance method (225 ± 5.2 mm, amounting to 87.9% of the total W_c) (Table 2). ET_a and *ET* did not differ significantly from each other.

T_c was the largest water-balance component; total annual T_c for *C. mongolicum* was about 166 mm, accounting for 63.9% of total W_c during the growing period for the three years. The maximum T_c occurred in July, and the values in the summer (June, July, and August) were significantly higher than all other months. E_g was also a significant part of the water budget, totaling 81 ± 10 mm and accounting for 31.3% of total W_c during the growing period. There was good agreement between the magnitude of E_g and the monthly variation in ET_a. E_l was the smallest component of *ET*; its total of 9 ± 1 mm accounted for 3.2% of total W_c during the growing period.

Soil water storage (Δ*SWC*) occurred as a consequence of the infiltration and accumulation of water in deep soil layers. The monthly average Δ*SWC* was −0.7 ± 0.2 mm, for a total decrease in mean storage of −4 ± 1.0 mm during the growing period. This net loss during the growing season was offset by inputs of water from melting snow during the dormant season.

Groundwater use by vegetation (GW_r) averaged 155 ± 13 mm for the three years and accounted for 60.6% of total W_c during the growing period. In arid regions, precipitation is rare. Lateral seepage from the irrigation of oasis farmland and the continental river (Heihe River) provides a sufficient water source for groundwater recharge in this desert–oasis ecotone in the middle of China's Heihe River basin. Consequently, groundwater is the largest source of water for plants and is absorbed by plants to maintain their survival.

The total W_c of *C. mongolicum* at a community scale was 256 ± 4 mm annually. W_c was greatest in July, followed by August, June, September, May, and October. W_c in the summer was significantly higher than other seasons (P < 0.01).

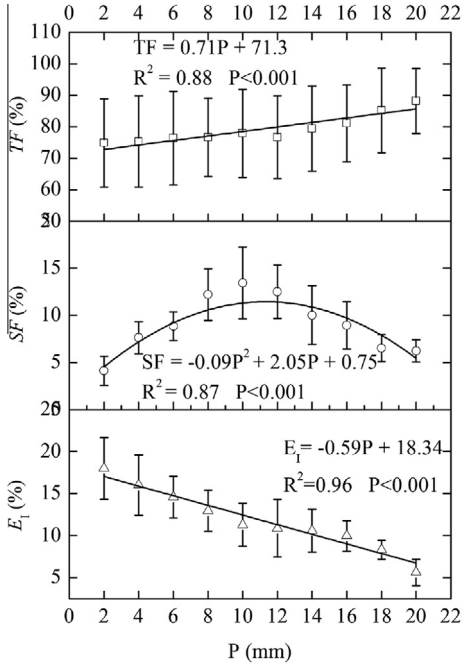

Fig. 6. The relationships between precipitation (*P*) and the partitioning of rainfall into throughfall (*TF*), stemflow (*SF*), and canopy interception (E_I) by desert shrubs.

4. Discussion

4.1. Effects of environmental variables on evapotranspiration partitioning

To accurately predict the response of ecosystem processes to climate change, it is necessary to accurately partition *ET* and determine the effects of environmental variables (Williams et al., 2004; Lauenroth and Bradford, 2006; Hu et al., 2009) on these individual processes. In our study, the good fits found for *ET*, T_c, and E_g with functions for R_n and *VPD* ($R^2 > 0.83$) (Fig. 7, Table 3) indicated that R_n and *VPD* played an important role in determining *ET*, T_c, and E_g. Furthermore the observed sensitivity of T_c to *VPD* confirmed the results of previous studies (Bush et al., 2008; Whitley et al., 2013; Peters et al., 2010; Litvak et al., 2012). Although the change in *ET* was in good agreement with that of *T*, the effects of *T* on the individual components of *ET* were not significant (Table 3). This suggests that the impact of small changes in *T* on *ET* may not be significant in this arid desert ecosystem, presumably because acclimation to hot conditions has already occurred. However, this does not preclude an indirect influence of *T* via associated changes in R_n, wind speed, and *VPD* (Eamus et al., 2013a).

In theory, the energy flux leaving the soil surface should be equivalent to the energy flux received at the surface over an ideal (non-vegetated) horizontal surface. However, studies have indicated that the available energy (net radiation minus soil heat flux) is generally greater than the sum of the vertical turbulent heat fluxes (sensible heat plus latent heat flux) (Wang and Zhang, 2011). In fact, the ratio of heat fluxes to available energy, which is often called the closure ratio, ranges from 70% to 90% for various ecosystems (Cava et al., 2008; Jacobs et al., 2008).

Groundwater is the store of water in the saturated zone beneath the ground surface (Chen et al., 2013). As the depth to groundwater increased from 4.1 to 6.4 m, total *ET*, E_c, and E_g declined linearly. An increasing depth to groundwater reduced the availability of this water supply to both vegetation and the ground surface, thereby causing the observed decline in *ET*, E_c, and E_g. In contrast, *ET* and T_c increased and then decreased as *SWC* increased across the range 1.1–3.1% (Fig. 7D). This may reflect the influence of increased shade and a reduced *VPD* on transpiration associated with the largest values of *SWC*, which arise after large rather than small rainfall events (Eamus et al., 2013b). Soil evaporation increased approximately linearly with increasing *SWC* across the entire range of *SWC*, reflecting the reduced resistance to diffusional loss of soil water when surface soils are wet.

An evaporating soil–plant surface is a dynamic system that is in constant interaction with the atmosphere and the interior of the soil. Although potential evapotranspiration (E_p) represents an upper limit to *ET* from a wet soil–plant surface, *ET* is complex and is primarily controlled by the demand and supply of water and energy. Previous research found that the relationship between *ET* and E_p applied to the complementary theory in drier areas, i.e., E_p increases while *ET* decreases when a surface dries from initially wet conditions, the decreasing *ET* energy will be used to increase E_p, and the rate increase (or decrease) is equal. Our research showed that *ET* increased with the increase of E_p but the correlation was not significant ($R^2 = 0.38$; Fig. 8A), and that E_p decreased with increasing precipitation while *ET* changed little (Fig. 8B). However, *ET* declined linearly with a depth to groundwater increase (Fig. 7C), and *ET* increased and then decreased as *SWC* increased (Fig. 7D). This indicates that the coupling of groundwater and soil water content play an important role in regulating *ET* in a desert ecosystem in China. In addition, *ET* in September, when maximum precipitation is significantly less than that in June, July, and August, and net radiation show a similar trend, which suggests that the decrease in *ET* may be due to the decrease in available energy in September.

Table 2
Measured and estimated components of water balance for average of three years in the desert *C. mongolicum* ecosystem of China.

Month	Length (days)	*P* (mm)	E_I (mm)	T_c (mm)	E_g (mm)	ET_a (mm)	*ET* (mm)	Δ*SWC* (mm)	GW_r (mm)	W_c (mm)
May	31	14.8 ± 5.5bc	1.2 ± 0.5 bc	26.7 ± 0.5bc	9.8 ± 3.2bc	37.7 ± 3.6bc	34.8 ± 3.4bc	0.8 ± 0.0a	22.2 ± 3.6b	37.0 ± 3.6c
June	30	5.6 ± 0.2d	0.5 ± 0.0d	32.7 ± 2.3ab	13.6 ± 3.3ab	46.7 ± 4.9ab	42.7 ± 4.8ab	−1.1 ± 0.7b	42.2 ± 5.4a	47.8 ± 5.4abc
July	31	19.2 ± 10.2bc	1.5 ± 0.8 bc	35.2 ± 2.1a	17.4 ± 2.7ab	54.2 ± 4.9a	40.0 ± 0.9ab	−0.7 ± 0.2ab	35.7 ± 4.9a	54.9 ± 4.9a
August	31	16.6 ± 5.8bc	1.3 ± 0.5 bc	33.3 ± 3.1ab	18.5 ± 1.3a	53.2 ± 1.9a	47.1 ± 3.8a	−0.6 ± 0.2ab	37.3 ± 2.2a	53.8 ± 2.2ab
September	30	39.8 ± 18.1a	3.2 ± 1.5a	24.8 ± 3.1c	14.8 ± 0.3ab	42.8 ± 1.4ab	40.4 ± 4.1ab	0.8 ± 0.3a	2.3 ± 1.7c	42.1 ± 1.7bc
October	15	4.7 ± 1.3d	0.4 ± 0.1d	10.6 ± 1.7d	5.8 ± 1.3c	16.8 ± 2.5c	16.3 ± 3.3c	−3.4 ± 0.8c	15.4 ± 3.3b	20.2 ± 3.3d
Total	168	111 ± 9	9 ± 1	166 ± 6	81 ± 10	251 ± 8	225 ± 5.2	−4 ± 1.0	155 ± 13	256 ± 4
Proportion of total W_c (%)	39.4	3.2	63.9	31.3	98.3	87.9	1.7	60.6	100.0	

Variable names: Precipitation (*P*), interception (E_I), canopy transpiration (T_c), soil evaporation (E_g), actual evapotranspiration ($ET_a = E_I + E_c + E_g$), evapotranspiration (*ET*), soil water storage (Δ*SWC*), groundwater use by the vegetation ($GW_r = ET_a - P - \Delta SWC$), water consumption ($W_c = P + GW_r$) is that the water requirements in actual can maintain the ecosystem stability in natural environment, which it equal the total of groundwater recharge and precipitation, including actual evapotranspiration, and soil water storage. Means for a parameter followed by different letters differ significantly (Tukey's HSD, $P < 0.05$). Values are means ± SEM.

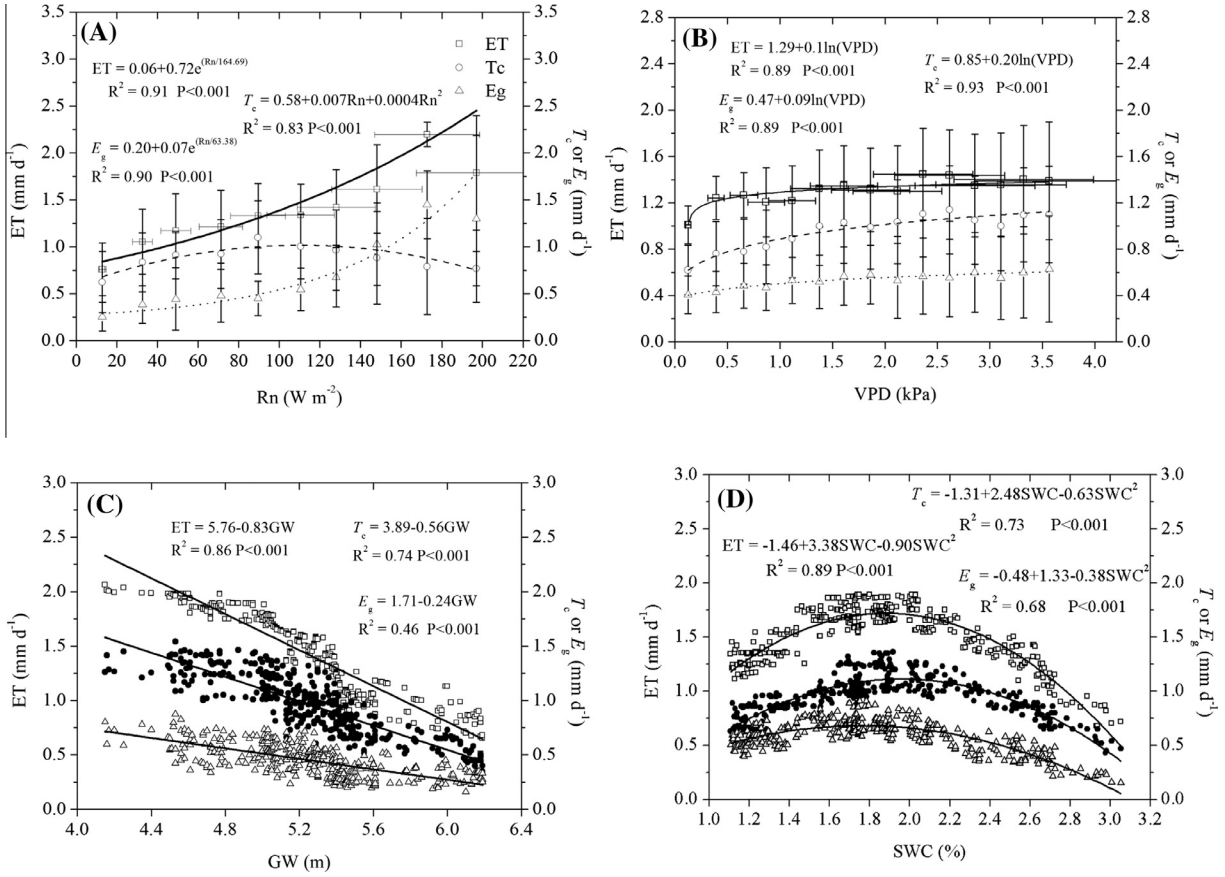

Fig. 7. The relationship between actual evapotranspiration (*ET*), canopy transpiration (T_c), and soil evaporation (E_g) and (A) net radiation (R_n), (B) vapor pressure deficit (*VPD*), (C) groundwater depth (*GW*), and (D) soil water content (*SWC*).

Table 3
Degrees of freedom and *F*-statistics for the repeated-measurement ANOVA on the effects of environmental variables and their interactions on canopy transpiration (T_c), soil evaporation (E_g), evapotranspiration (*ET*), canopy conductance (g_c), and community conductance (g_S) during the growing period.

Factor	*df*	T_c	E_g	*ET*	g_c	g_s
VPD	4	8.4***	4.4**	6.4***	7.7***	4.3**
T	2	0.2	0.3	0.5	2.7	2.8
SWC	2	9.8***	6.8**	3.5*	26.3***	6.6**
R_n	4	3.8**	16.7***	8.3***	2.8*	0.8
VPD × *T*	2	3.2*	0.8	2.9	4.5**	0.7
VPD × *SWC*	6	0.8	1.8	2.3*	10.0***	0.3
T × *SWC*	3	0.6	1.0	0.4	2.1	1.2
VPD × *T* × *SWC*	3	0.2	1.0	0.4	1.8	1.7
VPD × R_n	8	0.9	2.3*	1.5	4.6***	0.6
T × R_n	5	0.2	0.7	0.5	1.0	0.9
VPD × *T* × R_n	2	1.0	0.1	1.1	1.2	0.5
SWC × R_n	6	0.6	1.5	1.7	11.6***	1.0
VPD × *SWC* × R_n	9	0.8	1.2	1.4	7.8***	1.4
T × *SWC* × R_n	5	2.1	0.9	1.7	0.5	2.4*
VPD × *T* × *SWC* × R_n	9	0.7	1.3	1.9	6.6***	2.4*

* $P < 0.05$.
** $P < 0.01$.
*** $P < 0.001$.

The decoupling coefficient (Ω) increased from May to October and then decreased to its minimum value in December, its daily average throughout the year was 0.16, with maximum values of 0.36 in August (Fig. 9). The low values of Ω indicate that the *ET* should be coupled with the surface conductance (which is actually determined by the soil water availability) rather than available energy, so that water availability also played the dominate role in controlling the *ET* during the growing period.

Vegetation affects the seasonal partitioning of water and energy fluxes in arid ecosystems (Mendez-Barroso et al., 2014), principally through the seasonality of LAI (Barbour et al., 2005; Zhao and Liu, 2010; Liu et al., 2011, 2012). The limited water availability at the study site resulted in a low LAI of *C. mongolicum* (1.0 ± 0.3 m^2 m^{-2}; Fig. 10), which clearly contributed to the relatively low values of T_c. As expected, both T_c and *ET* increased logarithmically with increasing LAI (Fig. 10A); this was in contrast to the linear correlation previously found for *Caragana microphylla* (Yue et al., 2008). The relationship between LAI and g_c and g_s also showed an increasing trend (Fig. 10B). As LAI increased, the ratio of T_c/ET also increased, reflecting both an increased contribution of transpiration through leaves and a declining E_g from increased shading of the soil surface with increased LAI.

4.2. Sensitivity of stomatal conductance at canopy and community scales

Stomata are the primary location of active regulation of both CO_2 and water vapor fluxes through leaves (McCulloh and Woodruff, 2012). Stomatal sensitivity to *VPD* can be quantified as the magnitude of the response of stomatal conductance to increasing *VPD* relative to a reference conductance at *VPD* = 1 kPa (Oren et al., 1999a). In arid regions, stomatal sensitivity varies greatly within and between species and between scales due to a change in *VPD* (Ewers et al., 2005; Bovard et al., 2005; McCulloh and Woodruff, 2012) from 11 mm s^{-1} (*Picea abies*) to 147 mm s^{-1} (*Ephedra nevadensis*), and the extrapolated *VPD* at which the stomata close completely can range from 3.1 kPa (*Quercus alba*) to 12 kPA (*Larrea tridentata*) (Oren et al., 1999a, 2001; McCulloh

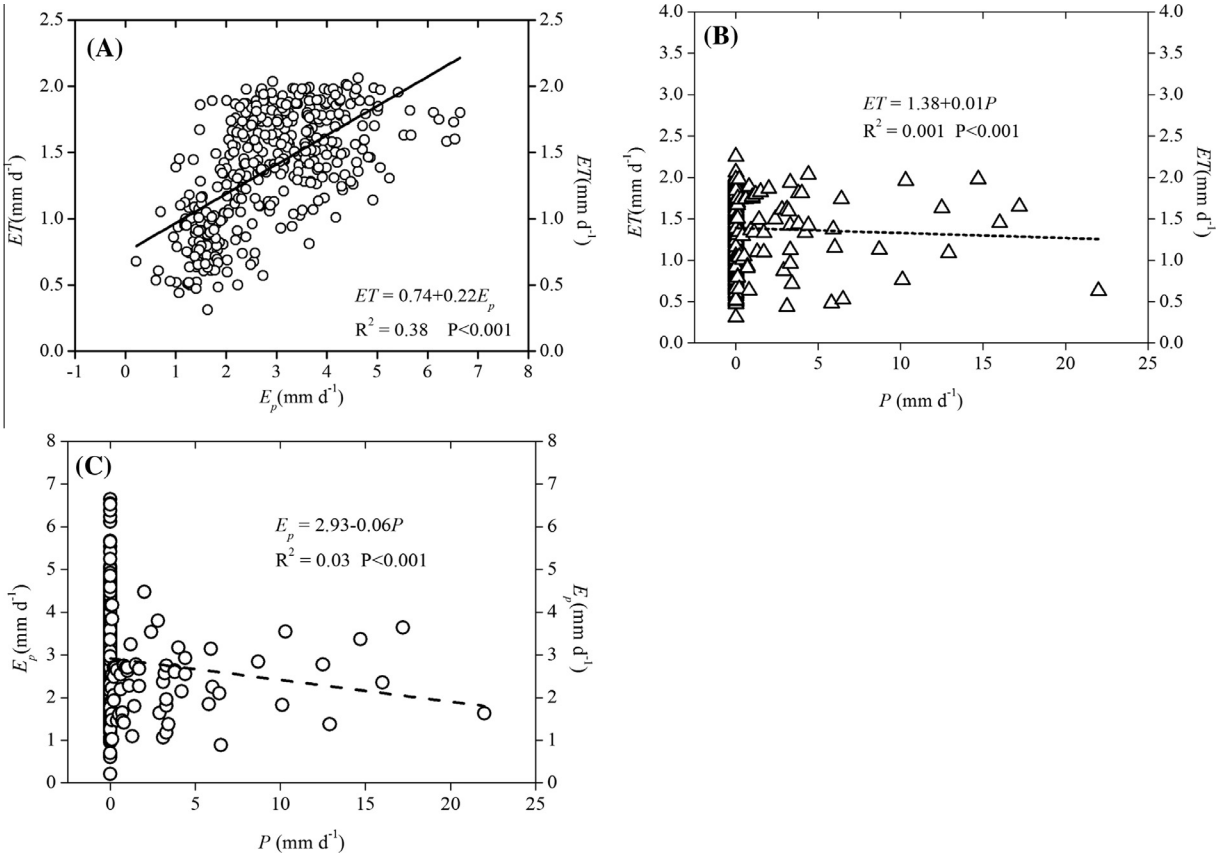

Fig. 8. The relationship between (A) evapotranspiration (*ET*) and potential evapotranspiration (E_p) in the mean daily; (B) evapotranspiration (*ET*) and precipitation (*P*); and (C) potential evapotranspiration (E_p) and precipitation in the mean daily.

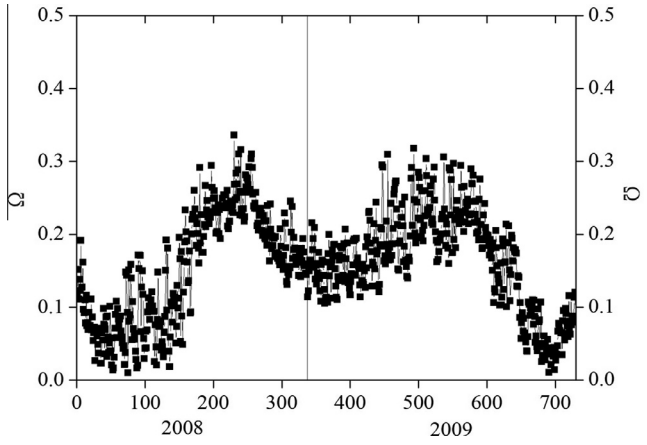

Fig. 9. Seasonal variations in decoupling coefficient (Ω) throughout the year from 2008 to 2009.

and Woodruff, 2012). The present study showed that stomatal sensitivity of *C. mongolicum* was 243.7 and 319.7 mm s^{-1} at the canopy and community scales, respectively (Fig. 10A), which was higher than that observed in *E. nevadensis*, *Q. alba*, and *L. tridentata* (Oren et al., 1999a, 2001; McCulloh and Woodruff, 2012). However, the extrapolated *VPD* at which stomatal closure occurred for *C. mongolicum* was similar to those of other drought-tolerant species, such as *E. nevadensis* (Oren et al., 1999a,b; Pataki et al., 2000; Ogle and Reynolds, 2002) and *Bothriochloa ischaemum* (Maherali et al., 2003). Simultaneously, the interactions of $VPD \times T \times SWC \times R_n$ on g_c were significant ($P < 0.001$, Table 3) but were not significant for g_s, indicating that the stomata of these desert shrubs were more sensitive at a canopy scale. The difference was likely due to the limits on water loss by different hydraulic architectures at different scales (Tyree and Zimmermann, 2002).

Stomatal closure occurs as a feedback response (Eamus et al., 2008) to transpiration and can exhibit both an increase in transpiration rate with increasing *VPD* for low-to-moderate values of *VPD* and in many cases a decrease in transpiration at high *VPD* (Monteith, 1995; Meinzer et al., 1997; Thomas and Eamus, 1999; Taneda and Sperry, 2008). In the present study, stomatal conductance increased with increasing *ET* and T_c at both scales ($R^2 = 0.96$ and $R^2 = 0.88$; Fig. 11B), but the role of stomata in regulating T_c during the closure response was linked more to *ET* than to *VPD* because of the lower values extrapolated for *ET* and T_c (0.2 and 0.1 mm d^{-1}, respectively), as has been observed previously (Monteith, 1995; Eamus et al., 2008). The improvement of water-use efficiency at high *VPD* is an important insight into the adaptive mechanisms of desert shrubs in arid environments. In addition, groundwater also plays an important role in water and energy fluxes. Our study showed that groundwater had a linear correlation with g_c and g_s, and the significance between *GW* and g_c ($R^2 = 0.86$) was greater than that between *GW* and g_s ($R^2 = 0.66$) (Fig. 11C). The variation in *SWC* was significantly expressed as a polynomial function of g_s ($R^2 = 0.85$) but was not significant with g_c (Fig. 11D). This suggests that groundwater strongly affects g_c, while soil water content has more influence on g_S in arid regions.

4.3. Components of the water balance

Precipitation events in this region are characterized as rainfall pulses with discontinuous, highly variable, and largely unpredictable frequency and intensity (Zhao and Liu, 2010). The desert

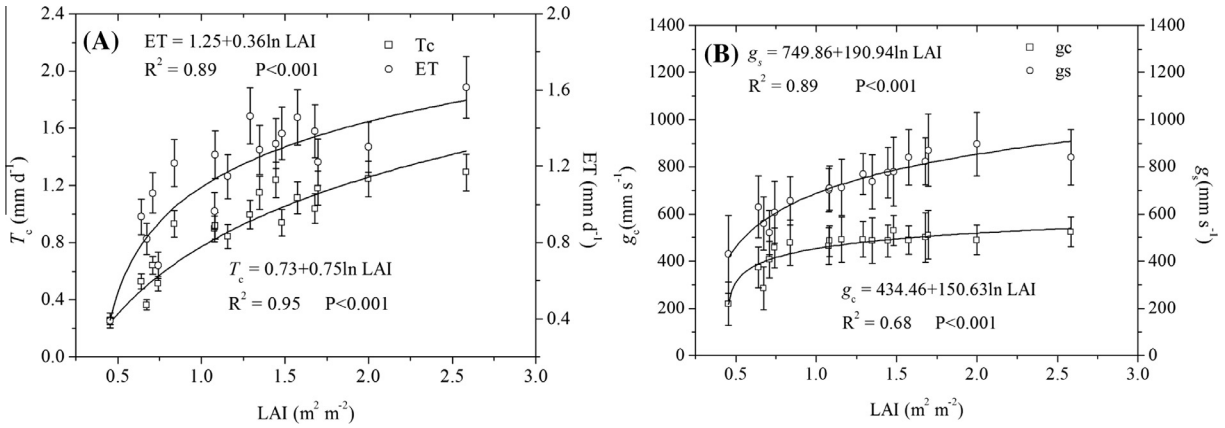

Fig. 10. The relationship between leaf area index (LAI) and (A) evapotranspiration (*ET*) and canopy transpiration (T_c) and (B) canopy conductance (g_c) and community conductance (g_S).

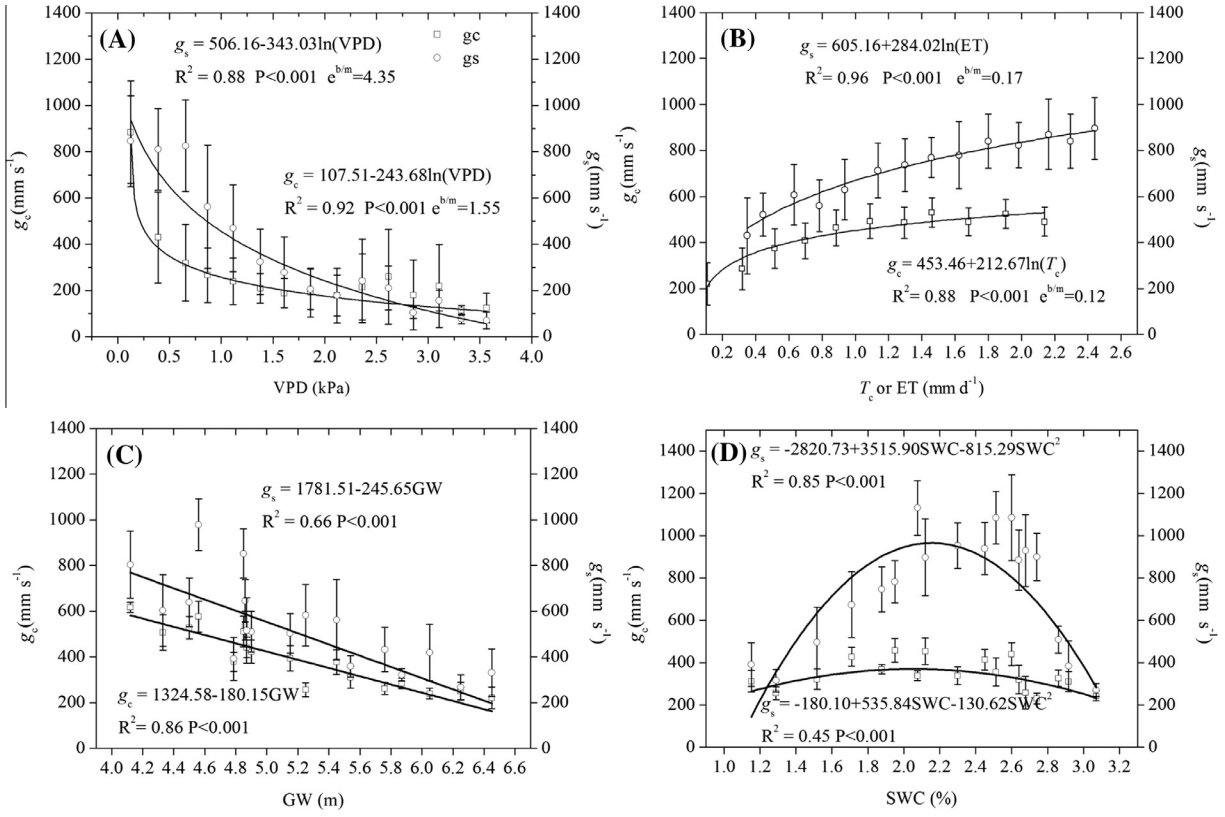

Fig. 11. The sensitivity of canopy conductance (g_c) and community conductance (g_s) to (A) vapor pressure deficit (*VPD*), (B) evapotranspiration (*ET*) or canopy transpiration (T_c), (C) groundwater depth (*GW*), and (D) soil water content (*SWC*).

regions of China usually experience small precipitation events (i.e., ⩽5 mm), and significant infiltration below the topsoil only occurs during periods of large and frequent precipitation (Fig. 2F and G). Large and infrequent precipitation events that lead to infiltration deep enough to increase root uptake have a marked effect on T_c (Zhao and Liu, 2010) and on aboveground biomass (Eamus, 2001; Knapp et al., 2008), as has been reported previously for other dry ecosystems (e.g., Tietjen et al., 2009; Raz-Yaseef et al., 2012).

Loss of water through *ET* represents either the largest (where significant groundwater uptake occurs) or the second largest component (where groundwater uptake does not occur and rainfall is therefore the largest single component) of the water balance in water-limited ecosystems. *ET* can account for more than 92.7% (or more than 100% if groundwater uptake occurs) of rainfall (Zhang et al., 2001; Wilcox and Thurow, 2006; Wang et al., 2010; Kool et al., 2014). In our study, ET_a accounted for more than 98.3% of water consumption. However, the differences in partitioning *ET* among canopy interception and soil evaporation factors are variable when the canopy is sparse because the spatial distribution of the components (E_l, E_g, and T_c) is more complex (Baldocchi et al., 2004); for example, the ratio T_c:*ET* varies greatly, ranging from 40% to 70% among ecosystems and time scales in water-limited environments (Scott et al., 2006; Cavanaugh et al., 2010; Staudt et al., 2011). A recent estimate of global *ET* partitioning from CLM3 was 41% T_c, 42% E_g, and 17% E_l (Lawrence et al., 2007). The large differences between the simulated results and observations from other studies may be due to the uncertainty of the model between regional and global scales.

In arid regions, the interaction between surface water and groundwater plays an important role in the ecohydrologic system and water-balance management (Sophocleous, 2002; Gilfedder et al., 2012). Generally, the river is the main recharge source of groundwater in the Heihe River Basin, and Tian et al. (2015) found that the net exchange from surface water to groundwater is 5.3×10^8 m^3 $year^{-1}$ in the river's main stream. However, river–aquifer interactions are often complicated by agricultural activities in midstream, including surface water diversion, groundwater pumping, and irrigation, as they could significantly alter the flow regimes of both surface water and groundwater (Tian et al., 2015; McCallum et al., 2013). Consequently, infiltration from river water and irrigation mainly occurs along land adjacent to the river and in agricultural areas in our study area; eventually, this water is consumed through evapotranspiration and crop absorption (Chen et al., 2006). River infiltration into the aquifers is about 4.4×10^8 m^3 $year^{-1}$ in the midstream and downstream regions, accounting for 27% of the mountainous runoff and 51% of the water flow in these sections of the river (Chen et al., 2006). In our study area, river leakage and groundwater discharge had a net exchange of 3×10^6 m^3 $year^{-1}$ (Tian et al., 2015). Since *C. mongolicum* is the dominant deep-rooted species in our desert–oasis ecotone study area (Liu and Zhao (2009)), it can absorb a large amount of groundwater (155 ± 13 mm $year^{-1}$) to compensate for the lack of annual precipitation (111 ± 9 mm), and to increases the ecosystem's resilience and shrub survival in arid regions of China.

5. Conclusions

Partitioning of evapotranspiration was affected by stomatal regulation, while the role of stomata in regulating canopy transpiration was correlated more with transpiration rates than vapor pressure deficit in arid regions. Although the response of evapotranspiration was strongly correlated with changes in air temperature, evapotranspiration is not sensitive to air temperature in this seasonally warm in a unique desert ecosystem. The stomata of desert shrubs at a canopy scale were more sensitive to water loss than at the community scale. Canopy transpiration was the dominant component of evapotranspiration, and rates of canopy water use exceeded rainfall because of the large uptake of groundwater by this deep-rooted shrub. Understanding the partitioning of evapotranspiration into its components will improve our understanding of the mechanisms that underlie adaptations of desert shrubs to aridity.

Acknowledgments

This study was supported by the National Outstanding Youth Funds of China (No. 41125002) and the National Natural Science Foundation of China (No. 41471024). We thank all the participants of the vegetation and environmental surveys conducted at the Linze Inland River Basin Research Station, Cold and Arid Regions Environmental and Engineering Research Institute, Chinese Academy of Sciences. The data used in this study are freely available from the corresponding author (Bing Liu, liubing@lzb.ac.cn) upon request. We also gratefully acknowledge the journal's anonymous reviewers for their valuable comments on an earlier version of our manuscript.

Appendix A. Supplementary material

Supplementary data associated with this article can be found, in the online version, at http://dx.doi.org/10.1016/j.jhydrol.2016.04.042. These data include Google maps of the most important areas described in this article.

References

Addington, R.N., Mitchell, R.J., Oren, R., Donovan, L.A., 2004. Stomatal sensitivity to vapor pressure deficit and its relationship to hydraulic conductance in *Pinus palustris*. Tree Physiol. 24, 561–569.

Allen, R.G., Pereira, L.A., Raes, D., Smith, M., 1998. Crop Evapotranspiration: Guidelines for Computing Crop Water Requirements. FAO Irrigation and Drainage Paper 56, FAO, Rome, Italy, p. 293.

Allen, R.G., Pereira, L.S., Howell, T.A., Jensen, M.E., 2011a. Evapotranspiration information reporting: I. Factors governing measurement accuracy. Agric. Water Manage. 98, 899–920.

Allen, R.G., Pereira, L.S., Howell, T.A., Jensen, M.E., 2011b. Evapotranspiration information reporting: II. Recommended documentation. Agric. Water Manage. 98, 921–929.

Austin, A.T., Yahdjian, L., Stark, J.M., Belnap, J., Porporato, A., Norton, U., Ravetta, D. A., Schaeffer, S.M., 2004. Water pulses and biogeochemical cycles in arid and semiarid ecosystems. Oecologia 141, 221–235.

Baldocchi, D.D., Xu, L.K., Kiang, N., 2004. How plant functional-type, weather, seasonal drought, and soil physical properties alter water and energy fluxes of an oak–grass savanna and an annual grassland. Agric. For. Meteorol. 123, 13–39.

Barbour, M.M., Hunt, J.E., Walcroft, A.S., Rogers, G.N.D., McSeveny, T.M., Whitehead, D., 2005. Components of ecosystem evaporation in a temperate coniferous rainforest, with canopy transpiration scaled using sapwood density. New Phytol. 165, 549–558.

Blanken, P.D., 2014. The effect of winter drought on evaporation from a high-elevation wetland. J. Geophys. Res. Biogeosci. 119, 1354–1369.

Bovard, B.D., Curtis, P.S., Vogel, C.S., Su, H.B., Schmid, H.P., 2005. Environmental controls on sap flow in a northern hardwood forest. Tree Physiol. 25, 31–38.

Bush, S.E., Pataki, D.E., Hultine, K.R., West, A.G., Sperry, J.S., Ehleringer, J.R., 2008. Wood anatomy constrains stomatal responses to atmospheric vapor pressure deficit in irrigated, urban trees. Oecologia 156, 13–20.

Cava, D., Contini, D., Donateo, A., Martano, P., 2008. Analysis of short-term closure of the surface energy balance above short vegetation. Agric. For. Meteorol. 148, 82–93.

Cavanaugh, M.L., Kurc, S.A., Scott, R.L., 2010. Evapotranspiration partitioning in semiarid shrubland ecosystems: a two-site evaluation of soil moisture control on transpiration. Ecohydrology 4, 671–681.

Caylor, K.K., D'Odorico, P., Rodriguez-Iturbe, I., 2006. On the ecohydrology of structurally heterogeneous semiarid landscapes. Water Resour. Res. 42, W07424. http://dx.doi.org/10.1029/2005WR004683.

Chang, X.X., Zhao, W.Z., Zhang, Z.H., Su, Y.Z., 2006. Sap flow of the Gansu Poplar shelter-belt in arid region of Northwest China. Agric. For. Meteorol. 138, 132–141.

Chen, Z.Y., Wan, L., Nie, Z.L., Shen, J.M., Chen, J.S., 2006. Identification of groundwater recharge in the Heihe Basin using environmental isotopes. Hydrol. Eng. Geol. 6, 9–14 (in Chinese with English abstract).

Chen, T.F., Wang, X.S., Li, H.L., Jiao, L.L., Wan, L., 2013. Redistribution of groundwater evapotranspiration and water table around a well field in an unconfined aquifer: a simplified analytical model. J. Hydrol. 495, 162–174.

Dai, A.G., 2011. Drought under global warming: a review. Clim. Change 2, 45–65.

Eamus, D., Taylor, D.T., Macinnis-Ng, C.M.O., Shanahan, S., De Silva, L., 2008. Comparing model predictions and experimental data for the response of stomatal conductance and guard cell turgor to manipulations of cuticular conductance, leaf-to-air vapor pressure difference and temperature: feedback mechanisms are able to account for all observations. Plant, Cell Environ. 31, 269–277.

Eamus, D., 2001. How does ecosystem water balance affect net primary productivity of woody ecosystems? Funct. Plant Biol. 30, 187–205.

Eamus, D., Boulain, N., Cleverly, J., Breshears, D.D., 2013a. Global change-type drought-induced tree mortality: vapor pressure deficit is more important than temperature per se in causing decline in tree health. Ecol. Evol. 3, 2711–2729.

Eamus, D., Cleverly, J., Boulain, N., Grant, N., Faux, R., Villalobos-Vega, R., 2013b. Carbon and water fluxes in an arid-zone acacia savanna woodland: an analyses of seasonal patterns and responses to rainfall events. Agric. For. Meteorol. 182–183, 225–238.

Ewers, B.E., Gower, S.T., Bond-Lamberty, B., Wang, C.K., 2005. Effects of stand age and tree species on canopy transpiration and average stomatal conductance of boreal forests. Plant, Cell Environ. 28, 660–678.

Gilfedder, M., Rassam, D.W., Stenson, M.P., Jolly, I.D., Walker, G.R., Littleboy, M., 2012. Incorporating land-use changes and surface–groundwater interactions in a simple catchment water yield model. Environ. Model. Softw. 38, 62–73.

Fischer, M., Kůcera, J., Deckmyn, G., Orsag, M., Sedlak, P., Žalud, Z., Ceulemans, R., 2013. Evapotranspiration of a high-density poplar stand in comparison with a reference grass cover in the Czech-Moravian Highlands. Agric. For. Meteorol. 118, 43–60.

Granier, A., Huc, R., Barigah, S.T., 1996. Transpiration of natural rain forest and its dependence on climatic factors. Agric. For. Meteorol. 78, 61–81.

Hu, Z.M., Yu, G.R., Zhou, Y.L., Sun, X.M., Li, Y.N., Shi, P.L., Wang, Y.F., Song, X., Zheng, Z.M., Zhang, L., Li, S.G., 2009. Partitioning of evapotranspiration and its controls in four grassland ecosystems: application of a two-source model. Agric. For. Meteorol. 149, 1410–1420.

Huxman, T.E., Wilcox, B.P., Breshears, D.D., Scott, R.L., Snyder, K.A., Small, E.E., Hultine, K., Pockman, W.T., Jackson, R.B., 2005. Ecohydrological implications of woody plant encroachment. Ecology 86, 308–318.

Jacobs, A.F.G., Heusinkveld, B.G., Holtslag, A.A.M., 2008. Towards closing the surface energy budget of a mid-latitude grassland. Bound-Lay. Meteorol. 126, 125–136.
Jarvis, P.G., McNaughton, K.G., 1986. Stomatal control of transpiration-scaling up from leaf to region. Adv. Ecol. Res. 15, 1–49.
Knapp, A., Beier, C., Briske, D., Classen, A., Luo, Y., Reichstein, M., Smith, M., Smith, S., Bell, J., Fay, P., Heisler, J., Leavitt, S., Sherry, R., Smith, B., Weng, E., 2008. Consequences of more extreme precipitation regimes for terrestrial ecosystems. Bioscience 58, 811–821.
Kool, D., Agam, N., Lazarovitch, N., Heitman, J.L., Sauer, T.J., Ben-Gal, A., 2014. A review of approaches for evapotranspiration partitioning. Agric. For. Meteorol. 184, 56–70.
Kurc, S.A., Small, E.E., 2004. Dynamics of evapotranspiration in semiarid grassland and shrubland ecosystems during the summer monsoon season, central New Mexico. Water Resour. Res. 40, W09305. http://dx.doi.org/10.1029/2004WR003068.
Lauenroth, W.K., Bradford, J.B., 2006. Ecohydrology and the partitioning AET between transpiration and evaporation in a semiarid steppe. Ecosystems 9, 756–767.
Law, B.E., Falge, E., Gu, L., Baldocchi, D., Bakwin, P., Berbigier, P., Davis, K., Dolman, A. J., Falk, M., Fuentes, J.D., Goldstein, A., Granier, A., Grelle, A., Hollinger, D., Janssens, I.A., Jarvis, P., Jensen, N.O., Katul, G., Mahli, Y., Matteucci, G., Meyers, T., Monson, R., Munger, W., Oechel, W., Olson, R., Pilegaard, K., Paw, U.K.T., Thorgeirsson, H., Valentini, R., Verma, S., Vesala, T., Wilson, K., Wofsy, S., 2002. Environmental controls over carbon dioxide and water vapor exchange of terrestrial vegetation. Agric. For. Meteorol. 113, 97–120.
Lawrence, D.M., Thornton, P.E., Oleson, K.W., Bonan, G.B., 2007. The partitioning of evapotranspiration into transpiration, soil evaporation, and canopy evaporation in a GCM: impacts on land-atmosphere interaction. J. Hydrometeorol. 8, 862–880.
Lei, H.M., Yang, D.W., 2010. Interannual and seasonal variability in evapotranspiration and energy partitioning over an irrigated cropland in the North China Plain. Agric. For. Meteorol. 150, 581–589.
Lindroth, A., Iritz, Z., 1993. Surface energy budget dynamics of short-rotation willow forest. Theor. Appl. Climatol. 47, 175–185.
Litvak, E., McCarthy, H.R., Pataki, D.E., 2012. Transpiration sensitivity of urban trees in a semi-arid climate is constrained by xylem vulnerability to cavitation. Tree Physiol. 32, 373–388.
Liu, B., Zhao, W.Z., 2009. Rainfall partitioning by desert shrubs in the arid regions. Sci. Cold Arid Reg. 1, 215–229.
Liu, B., Zhao, W.Z., Jin, B.W., 2011. The response of sap flow in desert shrubs to environmental variables in an arid region of China. Ecohydrology 4, 448–457.
Liu, C.W., Du, T.S., Li, F.S., Kang, S.Z., Li, S., Tong, L., 2012. Trunk sap flow characteristics during two growth stages of apple tree and its relationships with affecting factors in an arid region of northwest China. Agric. For. Meteorol. 104, 193–202.
Ma, N., Zhang, Y., Xu, C.Y., Szilagyi, J., 2015. Modeling actual evapotranspiration with routine meteorological variables in the data-scarce region of the Tibetan Plateau: comparisons and implications. J. Geophys. Res. Biogeosci. 120, 1638–1657.
Maherali, H., Johnson, H.B., Johnson, R.B., 2003. Stomatal sensitivity to vapor pressure difference over a subambient to elevated CO_2 gradient in a C_3/C_4 grassland. Plant, Cell Environ. 26, 1297–1306.
McCallum, A.M., Andersen, M.S., Giambastiani, B.M.S., Kelly, B.F.J., Ian Acworth, R., 2013. Rivereaquifer interactions in a semieardi environment stressed by groundwater abstraction. Hydrol. Process. 27, 1072–1085.
McCulloh, K.A., Woodruff, D.R., 2012. Linking stomatal sensitivity and whole-tree hydraulic architecture. Tree Physiol. 32, 369–372.
McDowell, N.G., White, S., Pockman, W.T., 2008. Transpiration and stomatal conductance across a steep climate gradient in the southern Rocky Mountains. Ecohydrology 1, 193–204.
Monteith, J.L., Unsworth, M.H., 1990. Principals of Environmental Physics, second ed. Edward Arnold, London.
Meinzer, F.C., Hinckley, T.M., Ceulemans, R., 1997. Apparent responses of stomata to transpiration and humidity in a hybrid poplar canopy. Plant, Cell Environ. 20, 1301–1308.
Mendez-Barroso, L.A., Vivoni, E.R., Robles-Morua, A., Mascaro, G., Yepez, E.A., Rodriguez, J.C., Watts, C.J., Garatuza-Payan, J., Saiz-Hernandez, J., 2014. A modeling approach reveals differences in evapotranspiration and its partitioning in two semiarid ecosystems in Northwest Mexico. Water Resour. Res. 50, 3229–3252.
Mitchell, P.J., Veneklaas, E., Lambers, H., Burgess, S.S.O., 2009. Partitioning of evapotranspiration in a semi-arid eucalypt woodland in south-western Australia. Agric. For. Meteorol. 149, 25–37.
Monteith, J.L., 1995. A reinterpretation of stomatal responses to humidity. Plant, Cell Environ. 18, 357–364.
Morana, M.S., Scotta, R.L., Keefera, T.O., Emmericha, W.E., Hernandeza, M., Nearingb, G.S., Paigec, G.B., Coshd, M.H., O'Neille, P.E., 2009. Partitioning evapotranspiration in semiarid grassland and shrubland ecosystems using time series of soil surface temperature. Agric. For. Meteorol. 149, 59–72.
Ogle, K., Reynolds, J.F., 2002. Desert dogma revisited: coupling of stomatal conductance and photosynthesis in the desert shrub, *Larrea tridentate*. Plant Cell Environ. 25, 909–921.
Oren, R., Phillips, N., Ewers, B.E., Pataki, D.E., Megonigal, J.P., 1999a. Sap-flux-scaled transpiration responses to light, vapor pressure deficit and leaf area reduction in a flooded *Taxodium distichum* forest. Tree Physiol. 19, 337–347.
Oren, R., Sperry, J.S., Ewers, B.E., Pataki, D.E., Phillips, N., Megonigal, J.P., 2001. Sensitivity of mean canopy stomatal conductance to vapor pressure deficit in a flooded *Taxodium distichum* L. forest: hydraulic and non-hydraulic effects. Oecologia 126, 21–29.
Oren, R., Sperry, J.S., Katul, G.G., Pataki, D.E., Ewers, B.E., Phillips, N., Schäfer, K.V.R., 1999b. Survey and synthesis of intra- and interspecific variation in stomatal sensitivity to vapor pressure deficit. Plant, Cell Environ. 22, 1515–1526.
Perez, P.J., Castellvi, F., Ibañez, M., Rosell, J.I., 1999. Assessment of reliability of Bowen ratio method for partitioning fluxes. Agric. For. Meteorol. 97, 141–150.
Pataki, D.E., Huxman, T.E., Jordan, D.N., Zitzer, S.F., Coleman, J.S., Smith, S.D., Nowak, R.S., Seemann, J.R., 2000. Water use of two Mojave Desert shrubs under elevated CO_2. Glob. Change Biol. 6, 889–897.
Peters, E.B., McFadden, J.P., Montgomery, R.A., 2010. Biological and environmental controls on tree transpiration in a suburban landscape. J. Geophys. Res. 115, G04006. http://dx.doi.org/10.1029/2009JG001266.
Raz-Yaseef, N., Yakir, D., Schiller, G., Cohen, S., 2012. Dynamics of evapotranspiration partitioning in a semi-arid forest as affected by temporal rainfall patterns. Agric. For. Meteorol. 157, 77–85.
Scott, R.L., Huxman, T.E., Cable, W.L., Emmerich, W.E., 2006. Partitioning of evapotranspiration and its relation to carbon dioxide exchange in a Chihuahuan Desert shrubland. Hydrol. Process. 20, 3227–3243.
Sophocleous, M., 2002. Interactions between groundwater and surface water: the state of the science. Hydrogeol. J. 10, 52–67.
Staudt, K., Serafimovich, A., Siebicke, L., Pyles, R.D., Falge, E., 2011. Vertical structure of evapotranspiration at a forest site (a case study). Agric. For. Meteorol. 151, 709–729.
Takagi, K., Tsuboya, T., Takahashi, H., 1998. Diurnal hystereses of stomatal and bulk surface conductances in relation to vapor pressure deficit in a cool-temperate wetland. Agric. For. Meteorol. 91, 177–191.
Taneda, H., Sperry, J.S., 2008. A case-study of water transport in co-occurring ring-versus diffuse-porous trees: contrasts in water status, conducting capacity, cavitation and vessel refilling. Tree Physiol. 28, 1641–1651.
Thomas, D.S., Eamus, D., 1999. The influence of predawn leaf water potential on stomatal responses to atmospheric water content at constant C_i and on stem hydraulic conductance and foliar ABA concentrations. J. Exp. Bot. 50, 243–251.
Tian, Y., Zheng, Y., Wu, B., Wu, X., Liu, J., Zheng, C.M., 2015. Modeling surface water-groundwater interaction in arid and semi-arid regions with intensive agriculture. Environ. Modell. Softw. 63, 170–184.
Tietjen, B., Zehe, E., Jeltsch, F., 2009. Simulating plant water availability in dry lands under climate change: a generic model of two soil layers. Water Resour. Res. 45. http://dx.doi.org/10.1029/2007WR006589.
Tyree, M.T., Zimmermann, M.H., 2002. Xylem Structure and the Ascent of Sap. Springer, Heidelberg, Germany.
Unland, H.E., Houser, P.R., Shuttleworth, W.J., Yang, Z.L., 1996. Surface flux measurement and modeling at a semi-arid Sonoran Desert site. Agric. For. Meteorol. 82, 119–153.
Wang, L.X., Caylor, K.K., Villegas, J.C., Barron-Gafford, G.A., Breshears, D.D., Huxman, T.E., 2010. Partitioning evapotranspiration across gradients of woody plant cover: assessment of a stable isotope technique. Geophys. Res. Lett. 37 (L09401), 2010. http://dx.doi.org/10.1029/2010GL043228.
Wang, R.Y., Zhang, Q., 2011. An assessment of storage terms in the surface energy balance of a subalpine meadow in Northwest China. Adv. Atmos. Sci. 3, 691–698.
Wilcox, B.P., Thurow, T.L., 2006. Emerging issues in rangeland ecohydrology: vegetation change and the water cycle. Rangel. Ecol. Manage. 59, 220–224.
Whitley, R., Taylor, D., Macinnis-Ng, C., Zeppel, M., Yunusa, I., O'Grady, A., Froend, R., Medlyn, B., Eamus, D., 2013. Developing an empirical model of canopy water flux describing the common response of transpiration to solar radiation and VPD across five contrasting woodlands and forests. Hydrol. Process. 27, 1133–1146.
Williams, D.G., Cable, W., Hultine, K., Hoedjes, J.C.B., Yepez, E.A., Simonneaux, V., Er-Raki, S., Boulet, G., de Bruin, H.A.R., Chehbouni, A., Hartogensis, O.K., Timouk, F., 2004. Evapotranspiration components determined by stable isotope, sap flow and eddy covariance techniques. Agric. For. Meteorol. 125, 241–258.
Wullschleger, S.D., Gunderson, C.A., Hanson, P.J., Wilson, K.B., Norby, R.J., 2002. Sensitivity of stomatal and canopy conductance to elevated CO_2 concentration—interacting variables and perspectives of scale. New Phytol. 153, 485–496.
Yue, G., Zhao, G., Zhang, T., Zhao, X.Y., Niu, L., Drake, S., 2008. Evaluation of water use of *Caragana microphylla* with the stem heat-balance method in Horqin Sandy Land, Inner Mongolia, China. Agric. For. Meteorol. 148, 1668–1678.
Zhang, L., Dawes, W.R., Walker, G.R., 2001. Response of mean annual evapotranspiration to vegetation changes at catchment scale. Water Resour. Res. 37, 701–708.
Zhao, W.Z., Chang, X.L., 2014. The effect of hydrological processes change on NDVI of desert–oasis ecotone in Hexi corridor of China. Sci. China Ser. D 7, 1561–1571.
Zhao, W.Z., Liu, B., 2010. The response of sap flow in shrubs to rainfall pulses in the desert region of China. Agric. For. Meteorol. 150, 1297–1306.
Zhu, G.F., Lu, L., Su, Y.H., Wang, X.F., Cui, X., Ma, J.Z., He, J.H., Zhang, K., Li, C.H., 2014. Energy flux partitioning and evapotranspiration in a sub-alpine spruce forest ecosystem. Hydrol. Process. 28, 5093–5104.